

RESEARCH

Open Access



Diagnostic and prognostic performance of serum GPC3 and PIVKA-II in AFP-negative hepatocellular carcinoma and establishment of nomogram prediction models

Yingying Lin^{1†}, Yuefei Ma^{2,3†}, Yan Chen¹, Yepei Huang¹, Jinchuan Lin^{2,3}, Zhenzhou Xiao^{1*} and Zhaolei Cui^{1*}

Abstract

Objective A significant proportion, ranging from 20 to 40%, of individuals with hepatocellular carcinoma (HCC) do not exhibit elevated Alpha-fetoprotein (AFP) levels. This study aimed to evaluate the utility of serum glypican-3 (GPC3) and protein induced by vitamin K absence or antagonist II (PIVKA-II) in an AFP-negative HCC (N-HCC) population, and to develop nomogram diagnostic and prognostic prediction models utilizing GPC3 and PIVKA-II.

Methods Serum GPC3 and PIVKA-II levels were measured in this case-control study, followed by the establishment of a receiver operating characteristic (ROC) curve, restricted cubic spline (RCS), and Kaplan-Meier survival curve. Additionally, a diagnostic prediction nomogram was constructed using univariate and multivariate logistic regression. Furthermore, we utilized least absolute shrinkage and selection operator (LASSO) regression and multivariate Cox regression to develop a prognostic prediction nomogram. The performance of these models was evaluated using ROC curve analysis and decision curve analysis (DCA).

Results Serum GPC3 and PIVKA-II expression levels were significantly elevated in untreated patients with N-HCC (especially stage and tumor size < 3 cm) compared to those with AFP-negative benign liver disease (N-BLD). Derived from ROC analysis, the diagnostic cutoff points for GPC3 and PIVKA-II were set at 0.100 ng/mL and 40.00 mAU/mL, respectively. PIVKA-II demonstrated sensitivity and specificity of 84.62% and 90.38%, surpassing GPC3's 76.92% and 73.08%. The area under the ROC curve (AUC) for a diagnostic prediction nomogram incorporating GPC3, PIVKA-II, and gamma-glutamyltransferase (GGT) was 0.943 (95% CI: 0.912–0.974), superior to models using GPC3 or PIVKA-II alone. This model showed 95.20% sensitivity and 81.70% specificity in differentiating N-HCC from N-BLD. Stratifying patients into high-risk and low-risk groups using cutoff values established by RCS for GPC3 (0.124 ng/mL) and PIVKA-II (274 mAU/mL) revealed significant associations between these risk stratifications and patient survival. Finally, the use of GPC3-highrisk, cirrhosis, albumin (ALB), portal venous thrombosis (PVT), and surgical treatment as five parameters in

[†]Yingying Lin and Yuefei Ma contributed equally to this work.

*Correspondence:
Zhenzhou Xiao
xiaozhenzhou250272@fjmu.edu.cn
Zhaolei Cui
cuileidizi@fjmu.edu.cn

Full list of author information is available at the end of the article



© The Author(s) 2025. **Open Access** This article is licensed under a Creative Commons Attribution-NonCommercial-NoDerivatives 4.0 International License, which permits any non-commercial use, sharing, distribution and reproduction in any medium or format, as long as you give appropriate credit to the original author(s) and the source, provide a link to the Creative Commons licence, and indicate if you modified the licensed material. You do not have permission under this licence to share adapted material derived from this article or parts of it. The images or other third party material in this article are included in the article's Creative Commons licence, unless indicated otherwise in a credit line to the material. If material is not included in the article's Creative Commons licence and your intended use is not permitted by statutory regulation or exceeds the permitted use, you will need to obtain permission directly from the copyright holder. To view a copy of this licence, visit <http://creativecommons.org/licenses/by-nc-nd/4.0/>.

the nomogram prognostic prediction model effectively differentiated between high- and low-risk prognostic patients with N-HCC with relatively high accuracy.

Conclusions Serum GPC3 and PIVKA-II demonstrate clinical significance in the timely detection and prognosis assessment of N-HCC. The application of nomogram prediction models based on GPC3 and PIVKA-II stands as an important adjunctive tool for diagnosing and prognosticating N-HCC.

Keywords Glypican-3, Protein induced by vitamin K absence or antagonist II, Hepatocellular carcinoma, Diagnosis, Prognosis, Nomogram

Introduction

Hepatocellular carcinoma (HCC) persists as the third leading cause of cancer-related mortality worldwide, with its global incidence and associated mortality rates having increased by 27% and 25%, respectively, between 2010 and 2019 [1]. Recent epidemiological data from 2022 indicate that HCC accounted for approximately 865,000 new cases and 757,948 deaths globally, solidifying its position as a major contributor to cancer-related mortality [2]. As the predominant pathological subtype of liver cancer, HCC represents 70–90% of all primary liver malignancies [3]. The clinical presentation of HCC is particularly challenging due to its insidious onset [4]. During the early stages of HCC (characterized by tumor diameters of 3–5 cm), the majority of patients remain asymptomatic, resulting in approximately 80% of cases being diagnosed at advanced stages [5]. Even when detected in early stages, successful treatment outcomes are primarily limited to very early-stage cases, typically defined as single lesions measuring less than 2 cm [6]. Patients with advanced-stage HCC often present with extensive tumor invasion, leading to suboptimal treatment responses and a dismal 5-year overall survival rate of approximately 14.1% [7]. Consequently, the enhancement of early diagnostic accuracy, improvement of therapeutic efficacy, and development of novel prognostic evaluation methods for outcome prediction have emerged as critical challenges in the clinical management of HCC.

Alpha-fetoprotein (AFP) is the most commonly used serological marker for the screening and auxiliary diagnosis of HCC [8, 9]. Studies have demonstrated that AFP levels may increase several years before the clinical diagnosis of HCC [10, 11]. Other research has revealed that AFP combined with ultrasound detection provides a relatively better ability to detect early-stage HCC [8]. In contrast, studies report normal AFP levels in 20–40% of HCC patients using a serum cutoff of 20 ng/mL. Notably, the proportion of AFP-negative HCC (N-HCC) among patients with small HCC (< 3 cm) reaches approximately 40% [8, 12]. Our study indicates that N-HCC may constitute a distinct subclass of HCC, necessitating further thorough investigation. Characterized by concealed and atypical clinical manifestations, early diagnosis of N-HCC presents significant challenges [13]. Therefore,

relevant clinical guidelines and recommendations suggest using all available markers to improve the diagnostic accuracy of small HCC, especially by applying reliable biomarkers for diagnosing N-HCC [14].

Glypican-3 (GPC3), a cell surface-anchored proteoglycan, is attached to the plasma membrane through glycosyl-phosphatidylinositol linkage and functions as a crucial molecular regulator of various cellular processes, including proliferation, differentiation, migration, and adhesion [15, 16]. This molecule has emerged as a promising biomarker for HCC, demonstrating particular diagnostic value in both early HCC detection and differentiation from benign hepatic lesions [17, 18]. Numerous studies have consistently shown that serum GPC3 levels are significantly elevated in HCC patients compared to both healthy controls and individuals with liver cirrhosis [19, 20]. A comprehensive meta-analysis encompassing 11 studies using of liver cirrhosis cases as the control on serum GPC3, revealed the combination of GPC3 and AFP yielded a better sensitivity than GPC3 or AFP [21, 22]. Notably, emerging evidence suggests that approximately 40% of HCC patients exhibit GPC3 positivity while remaining AFP-negative [23], with no significant correlation observed between GPC3 and AFP expression levels [24].

Protein induced by vitamin K absence or antagonist II (PIVKA-II) is another useful HCC marker that has been successfully applied in clinical practice. Furthermore, the guidelines of the Japan Society of Hepatology [25] and the Asia-Pacific Association for the Study of the Liver [26] have recommended incorporating PIVKA-II into the screening strategy for high-risk groups of HCC. Studies have shown that PIVKA-II levels remain almost unchanged in benign liver diseases (BLD), while its sensitivity and specificity for diagnosing early HCC are superior to those of AFP [27, 28]. PIVKA-II monitoring can also reduce the missed detection rate of HCC [29, 30]. Research has demonstrated that PIVKA-II is not only beneficial for HCC diagnosis but can also be employed as a potential marker for predicting the prognosis of vascular infiltration, metastasis, and recurrence of HCC [31].

Although a few case-control studies on GPC3 or PIVKA-II in HCC diagnosis have been conducted both nationally and internationally, the clinical application

value of these two biomarkers in N-HCC has not been reported. Therefore, the novelty of the present case-control study, compared to all previous studies, lies in its exploration of the early diagnostic and prognostic value of these serological models in the N-HCC population, aiming to provide new strategies for their clinical implementation in N-HCC management.

Materials and methods

Participants

The study was approved by the Ethics Review Board of the Branch for Research and Clinical Technology Application, Ethics Committee of the Fujian Cancer Hospital (Approval No. SQ2015-049-01) and the First Affiliated Hospital of Fujian Medical University (Approval No. MRCTA, ECFAH of FMU [2017]019), and was conducted in accordance with the 1975 Declaration of Helsinki. Informed consent was obtained from all study participants prior to their enrollment.

The inclusion and exclusion criteria for participants were as follows: (1) Age exceeding 18 years, regardless of gender; (2) Absence of prior clinical treatment for liver disease prior to admission. No liver supportive therapy, such as medication or other therapeutic interventions, was permitted until study enrollment; (3) Availability of baseline liver function tests encompassing albumin (ALB), total bilirubin (TBIL), alanine aminotransferase (ALT), aspartate aminotransferase (AST), alkaline phosphatase (ALP), and γ -glutamyl transferase (GGT). Additionally, baseline serum AFP levels and imaging studies, such as helical computed tomography (CT), ultrasonography, magnetic resonance imaging (MRI), or biopsy-proven diagnosis, were required; (4) HCC diagnosis must align with the diagnostic criteria stipulated in the “Standard for Diagnosis and Treatment of Primary HCC (2019 Edition)” [32]; (5) Benign liver disease (BLD) encompassed patients with chronic hepatitis B and liver cirrhosis (with or without hepatitis B virus), with primary enrollment focused on patients with liver cirrhosis. Diagnosis adhered to the diagnostic criteria for liver diseases outlined in the “Guidelines for Prevention and Treatment of Chronic Hepatitis B (2019 Edition)” [33] and the “Chinese Guidelines on the Management of Liver Cirrhosis” [34]; (6) Willingness to provide blood samples meeting predefined specifications; and (7) Voluntary participation in this clinical trial, with comprehension of study procedures and prior provision of a signed, written informed consent; patients had to demonstrate the capability and willingness to adhere to study protocol procedures and visit requirements. Exclusion criteria included patients undergoing warfarin anticoagulant therapy, those diagnosed with alcoholic cirrhosis, or individuals with severe jaundice.

Instruments and reagents

The GPC3 level was measured manually with a PHOMO automatic quantitative microplate reader (Autobio) and a CanAg Glypican-3 chemiluminescence enzyme immunoassay (EIA) (Fujirebio Diagnostics AB) platform. The CanAg Glypican-3 EIA is an enzyme immunometric assay for the quantitative determination of GPC3 in human serum. Furthermore, an automatic immunoanalyzer (Lumipulse G1200) and Lumipulse G PIVKA-II (Fujirebio Inc.) were used to determine PIVKA-II levels. Lumipulse G 1200 is an assay system, including a set of immunoassay reagents, for the quantitative measurement of PIVKA-II in specimens based on coupled reaction-chemiluminescence enzyme immunoassay (CLEIA) technology by a two step sandwich immunoassay method on the Lumipulse G System. Both of them were estimated according to the relevant manufacturer’s instructions, and the calibrators and quality controls were carefully maintained.

Specimen collection and preparation

A total of 3 to 4 mL of venous blood were collected from patients either on the first or second day of hospitalization. The blood samples were collected into procoagulant tubes and allowed to stand at room temperature for 30 min. Subsequently, the samples were centrifuged at a speed of 3000 revolutions per minute (rpm) for a duration of 10 min. The resulting upper serum was then frozen in a refrigerator set at a temperature of -80°C . Assay samples within 4 h from thawing. Avoid successive freezing and thawing of specimens and avoid to use hemolyzed specimens.

Detection method of GPC3 and PIVKA-II

The serum samples, which initially exhibited baseline AFP levels, underwent subsequent analysis to determine the levels of GPC3 and PIVKA-II using enzyme-linked immunosorbent assay and chemiluminescence immunoassay techniques, respectively. The GPC3 assay employs a solid-phase, non-competitive 2-step immunoassay format, utilizing the direct sandwich technique with two mouse monoclonal antibodies targeting distinct epitopes within the GPC3 protein core. Conversely, the PIVKA-II immunoassay involves a two-step sandwich method, where an alkaline phosphatase (ALP)-labeled anti-prothrombin polyclonal antibody (rabbit) specifically interacts with PIVKA-II in immunocomplexes bound to particles coated with an anti-PIVKA-II monoclonal antibody (MU-3 antibody, mouse sourced).

The cutoff values for GPC3 and PIVKA-II in diagnosing N-HCC were not pre-established; instead, these cutoff points were determined post-hoc based on ROC analysis, which took into account both the sensitivity for

detecting N-HCC and the specificity for distinguishing it from N-BLD.

Follow-up of survival

The basic demographic and clinical data of HCC patients during their initial hospitalization were collected. This included information on gender, age, contact details, the method of tumor detection, Hepatitis B virus, baseline liver function tests (including ALB, TBIL, ALT, AST, ALP, and GGT), the presence or absence of cirrhosis, portal venous thrombosis (PVT), metastasis and ascites, tumor size, number of tumors, tumor stage (according to the 7th edition of tumor-node-metastasis staging established by the American Joint Committee on Cancer and the International Union Against Cancer) and treatment plan, among others. The living conditions of the patients were documented using electronic medical record inquiry and mobile phone contact. Follow-up assessments were conducted every 3 to 6 months to ensure the collection of updated treatment-related information. The follow-up period extended until either the occurrence of death or survival for a duration of three years from the time of admission. Participant follow-up remained ongoing as of March 2023.

Construction of a prognostic risk model

Univariate and multivariate logistic regression analyses were conducted to ascertain diagnostic predictors. Variables yielding a P value < 0.1 from the univariate analysis were incorporated into a multivariate logistic regression framework. Effect measures were derived using odds ratios (ORs) and their respective 95% confidence intervals (CIs). All selected features exhibited statistical significance and were subsequently utilized to construct the nomogram.

Prognostic predictors were initially screened using LASSO regression. Initially, LASSO analysis reduced the regression coefficients of variables to zero through the application of a penalized coefficient (λ). This approach excluded variables with zero regression coefficients while retaining those with non-zero coefficients. Subsequently, multivariate Cox regression analysis was employed to pinpoint independent prognostic factors, alongside their hazard ratios (HRs) and 95% CIs. Ultimately, a nomogram was formulated. The total score for the nomogram prediction models was computed by summing the point values assigned to each variable. These point values were obtained by drawing a vertical line from each variable axis to the corresponding point axis on the nomogram. The summed total score was then plotted on the total score scale. Model performance was assessed and optimized using cross-validation, bootstrap techniques, and other methodologies.

Model predictive capability was evaluated through ROC curve analysis, with an AUC of 0.75 or higher indicating satisfactory discrimination. Prediction accuracy was further scrutinized using calibration plots. Clinical utility was approximated via Decision Curve Analysis (DCA). All statistical tests were two-tailed, with $P \leq 0.05$ deemed statistically significant. The “rms” package, implemented in R version 4.4.2 (<http://www.r-project.org/>), was utilized for the development of the nomogram diagram.

Statistical analysis

GraphPad Prism (version 8.0.2) and SPSS (version 18.0) was employed for the purposes of data processing and statistical analysis. The χ^2 test or Fisher's Exact Test was utilized to analyze count data across various groups. Median (quartile) was used to represent quantitative data with a skewed distribution. The non-parametric Kruskal-Wallis rank sum test was employed to compare groups, while the non-parametric Mann-Whitney U test was used to compare between two groups. The plotting of the ROC curve for multivariate observation values and the calculation of the AUC were conducted using SPSS. Survival curves were generated using the Kaplan-Meier method and Log-rank method to compare survival rates. The calculation of survival rates was performed using R version 4.4.2. The HRs and 95% CIs were obtained using a RCS method by R (version 4.4.2) (<http://www.r-project.org/>).

Results

Basic demographic and clinical data of the participants

A total of 639 untreated patients were admitted to two medical centers from March 2018 to February 2020. Among the participants, 411 were diagnosed with HCC, and 228 were diagnosed with BLD. For group stratification based on AFP levels < 20 ng/mL, 104 HCC patients (25.3%) were categorized into the N-HCC study group, including 96 males and 8 females, with an age range of 34–80 years and a median age of 60.5 years. Additionally, 104 BLD patients with age and gender matching the N-HCC study group and AFP levels < 20 ng/mL were categorized into the N-BLD control group. The selection of participants is shown in Fig. 1. The demographic and clinical data of the participants are summarized in Tables 1 and 2.

Demographic and clinical characteristics analysis revealed significant differences between N-HCC and A-HCC groups. The N-HCC cohort demonstrated a significantly higher proportion of patients with specific clinical features, including advanced age (> 60 years), male gender, early-stage disease (stage I), small tumor size (< 3 cm), and non-metastatic status compared to the A-HCC group ($P < 0.05$; Table 1). Regarding the control

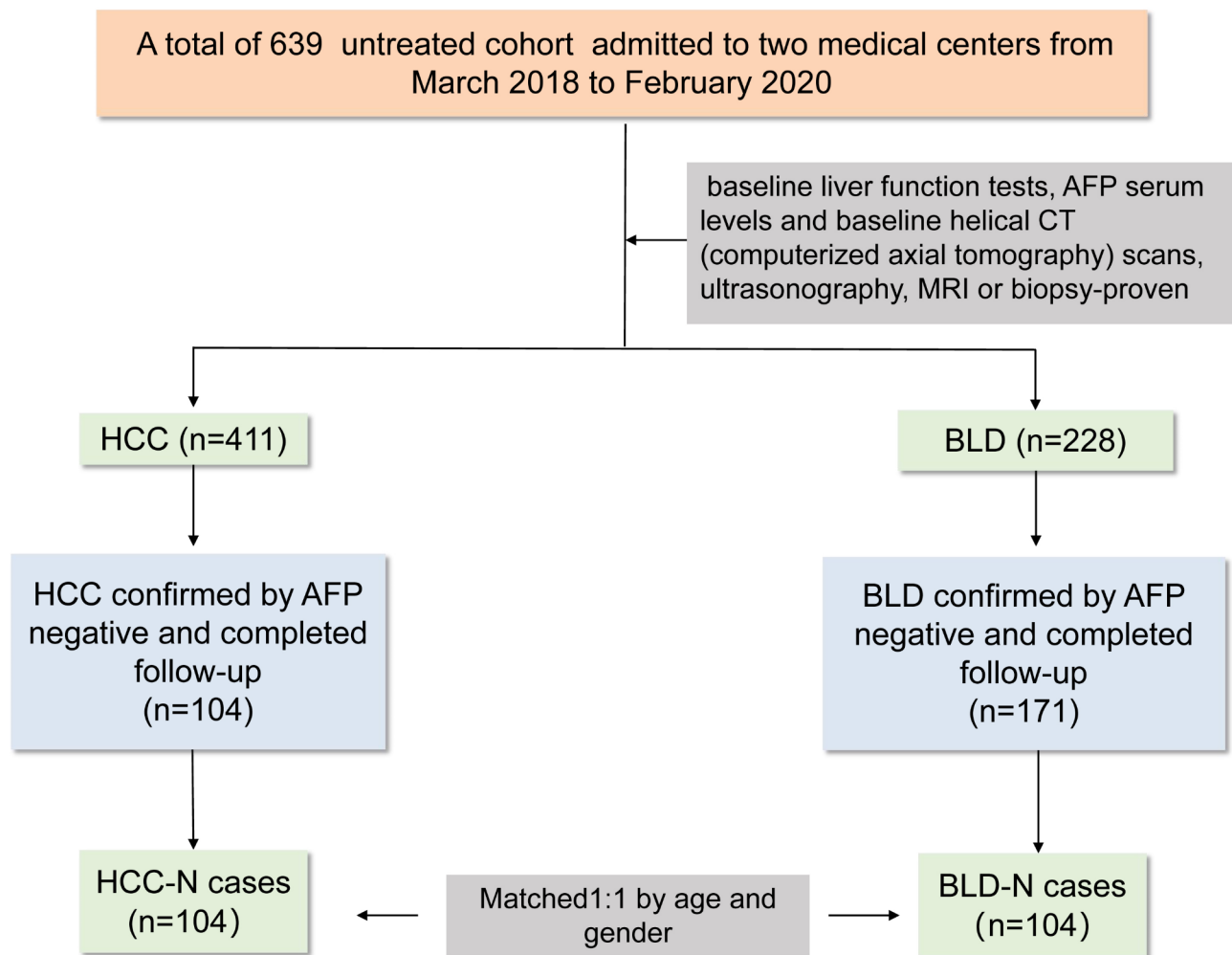


Fig. 1 Selection of Participants. HCC: hepatocellular carcinoma; BLD: benign liver disease

group, the 104 N-BLD patients were well-matched with the N-HCC group in terms of hepatitis B virus status and Child-Pugh classification. However, comparative analysis of liver function parameters showed that baseline liver function tests (excluding TBIL) in the N-BLD group were significantly lower than those observed in the N-HCC group ($P < 0.05$; Table 2).

Diagnostic value of GPC3 and PIVKA-II in N-HCC

The median serum levels of GPC3 (0.124 ng/mL) and PIVKA-II (274 mAU/mL) were significantly elevated in patients with N-HCC compared to those in the N-BLD group ($P < 0.05$; Fig. 2A and B). In stage I of N-HCC, the serum levels of GPC3 and PIVKA-II were significantly elevated compared to those in the N-BLD group ($P < 0.05$), yet remained significantly lower than those observed in stage IV of N-HCC ($P < 0.05$). Notably, no statistically significant differences were detected between stage I and stages II-III of N-HCC (Fig. 2C and D). Regarding tumor size differentiation, both GPC3 and

PIVKA-II demonstrated significant discriminatory power ($P > 0.05$) in distinguishing patients with small N-HCC (< 3 cm) from those with N-BLD. Furthermore, a positive correlation was observed between tumor size and biomarker levels, with both GPC3 and PIVKA-II concentrations showing progressive increases corresponding to larger tumor dimensions (Fig. 2E and F).

ROC curve analysis revealed distinct diagnostic performance for GPC3 and PIVKA-II in N-HCC detection (Fig. 2G and H). The AUC with 95% CI was 0.751 (0.684–0.819) for GPC3 and 0.925 (0.886–0.963) for PIVKA-II, respectively. Diagnostic evaluation using the optimal cutoff value of 0.100 ng/mL for GPC3, as determined by ROC analysis (Fig. 2G), demonstrated a sensitivity of 76.92%, specificity of 73.08%, and diagnostic accuracy of 50.00% (Table 3). Similarly, PIVKA-II analysis using the established cutoff value of 40 mAU/mL (Fig. 2H) showed superior diagnostic performance, with sensitivity, specificity, and accuracy rates of 84.62%, 90.38%, and 75.00%, respectively (Table 3).

Table 1 Basic demographic and clinical data of 411 patients with HCC

Clinical features	HCC(n = 411)	N-HCC(n = 104)	A-HCC (n = 307)	OR (95%CI)	P value
Age, n(%)					
≤ 60years	266 (64.72%)	52 (50.00%)	214 (69.71%)	301 (1.460–3.627)	0.000
> 60years	145 (35.28%)	52 (50.00%)	93 (30.29%)		
Gender, n(%)					
Male	356 (86.62%)	96 (92.31%)	260 (84.69%)	0.461 (0.210–1.011)	0.049
Female	55 (13.38%)	8 (7.69%)	47 (15.31%)		
Cirrhosis, n(%)					
Yes	267 (64.96%)	70 (67.31%)	197 (64.17%)	0.870 (0.543–1.394)	0.562
No	144 (35.04%)	34 (32.69%)	110 (35.83%)		
TNM stage, n(%)					
Stage I	76 (18.49%)	37 (35.58%)	39 (12.70%)	0.496 (0.389–0.633)	0.000
Stage II	75 (18.25%)	27 (25.96%)	48 (15.64%)		
Stage III	199 (48.42%)	30 (28.85%)	169 (55.05%)		
Stage IV	61 (14.84%)	10 (9.61%)	51 (16.61%)		
Tumor size, n(%)					
< 3 cm	59 (14.36%)	29 (27.89%)	30 (9.77%)	0.391 (0.289–0.530)	0.000
3–5 cm	116 (28.22%)	42 (40.38%)	74 (24.11%)		
> 5 cm	236 (57.42%)	33 (31.73%)	203 (66.12%)		
Daughter nodule, n(%)					
Yes	216 (52.55%)	49 (47.12%)	167 (54.40%)	0.747 (0.478–1.166)	0.199
No	195 (47.45%)	55 (52.88%)	140 (45.60%)		
Intrahepatic metastasis, n(%)					
Yes	209 (50.85%)	34 (32.69%)	175 (57.00%)	2.730 (1.710–4.358)	0.000
No	202 (49.15%)	70 (67.31%)	132 (43.00%)		
Distant metastasis, n(%)					
Yes	114 (27.74%)	21(20.19%)	93 (30.29%)	1.718 (1.004–2.939)	0.047
No	297 (72.26%)	83(79.81%)	214 (69.71%)		

HCC, hepatic cellular cancer. N-HCC, AFP-negative hepatic cellular cancer (AFP < 20 ng/mL). A-HCC, AFP-positive hepatic cellular cancer (AFP ≥ 20 ng/mL). N-HCC vs. A-HCC, were compared by the chi-square test or Fisher's exact test and $P < 0.05$ was statistically significant

Table 2 Basic demographic and clinical data of patients with N-BLD and N-HCC

Clinical features	N-BLD(n = 104)	N-HCC(n = 104)	OR(95%CI)	P value
Cirrhosis, n(%)	69 (66.35%)	70 (67.31%)	0.958 (0.538–1.706)	0.883
CHB, n(%)	35 (33.65%)	27 (25.96%)	1.447 (0.796–2.631)	0.225
Age ≤ 60years, n(%)	53 (50.96%)	52 (50.00%)	1.039 (0.603–1.790)	0.890
Male, n(%)	96 (92.31%)	96 (92.31%)	1.000 (0.361–2.733)	1.000
Hepatitis B virus, n(%)	94 (90.38%)	92 (88.46%)	1.226 (0.505–2.977)	0.652
Child- Pugh class A, n(%)	45 (43.27%)	45 (43.27%)	1.000 (0.578–1.731)	1.000
Child- Pugh class B, n(%)	53 (50.96%)	54 (51.92%)	0.962 (0.559–1.658)	0.890
ALB < 40 g/L, n(%)	40 (38.46%)	69 (66.35%)	0.317 (0.180–0.559)	0.000
TBIL > 21 μmol/L, n(%)	41 (39.42%)	30 (28.85%)	1.605 (0.900–2.863)	0.108
ALT > ULN, n(%)	18 (17.31%)	33 (31.73%)	0.450 (0.234–0.867)	0.016
AST > ULN, n(%)	34 (32.69%)	51 (49.04%)	0.505 (0.288–0.885)	0.016
ALP > ULN, n(%)	25 (24.04%)	42 (40.38%)	0.467 (0.257–0.848)	0.012
GGT > ULN, n(%)	37 (35.58%)	79 (75.96%)	0.175 (0.096–0.319)	0.000

N-BLD, AFP-negative benign liver disease (AFP < 20 ng/mL). N-HCC, AFP-negative hepatic cellular cancer (AFP < 20 ng/mL). CHB, Chronic Hepatitis B. ALB, albumin. TBIL, total bilirubin. ULN, upper limit of normal. ALT, aminoleucine transferase, ULN (male) = 50 μmol/L, ULN (female) = 40 μmol/L. AST, Aspartate aminotransferase, ULN (male) = 40 μmol/L, ULN (female) = 35 μmol/L. ALP, Alkaline Phosphatase, ULN (male) = 125 U/L, ULN (female) = 135 U/L. GGT, Gamma-glutamyltransferase, ULN (male) = 60 U/L, ULN (female) = 45 U/L

N-BLD vs. N-HCC, were compared by the chi-square test or Fisher's exact test, and $P < 0.05$ was statistically significant

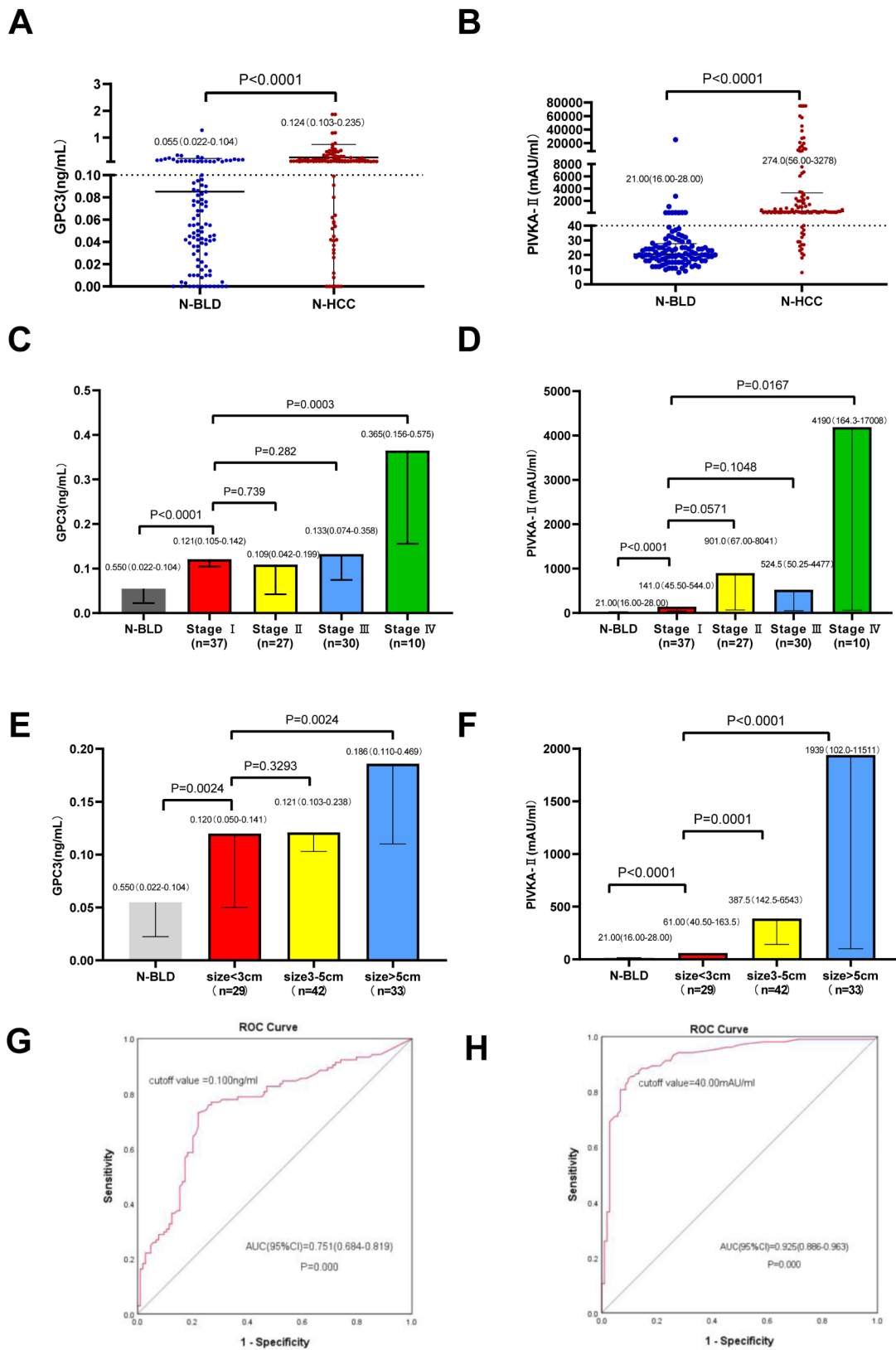


Fig. 2 (See legend on next page.)

(See figure on previous page.)

Fig. 2 Expression of GPC3 or PIVKA-II in N-HCC and N-BLD cohorts. **(A)** Comparative analysis of GPC3 expression between N-BLD and N-HCC cohorts. **(B)** Expression of PIVKA-II among the N-BLD and N-HCC cohorts. **(C)** Stage-specific variations in GPC3 expression across clinical stages. **(D)** Expression of PIVKA-II among the N-BLD and N-HCC groups in different stages. **(E)** Tumor size-dependent modulation of GPC3 biomarker profiles. **(F)** Expression of PIVKA-II among the N-BLD and N-HCC groups in different tumor size. **(G)** Diagnostic performance of GPC3 through ROC curve analysis. **(H)** Predictive accuracy assessment of PIVKA-II using ROC curve evaluation

Risk factors selection based on GPC3 and PIVKA-II and a nomogram diagnostic prediction model construction

All enrolled patients were randomly divided into development ($n=145$) and validation sets ($n=63$) with a proportion of 7: 3. In the two cohorts, eight continuous variable parameters—GPC3, PIVKA-II, ALB, TBIL, ALT, AST, ALP, and GGT—were dichotomized into binary variables based on their respective cutoff values (0: negative, 1: positive). First, we preliminarily selected predictors of N-HCC using univariate logistic regression analyses (Fig. 3A). Second, we included six predictors identified through multivariable logistic regression as independent risk variables to construct a prediction model. Among these, three predictors were found to be significant: GPC3 (OR=4.09, 95% CI: 1.6–10.54), PIVKA-II (OR=50.25, 95% CI: 19.07–160.87), and GGT (OR = 8.81, 95% CI: 3.27–28.32) (Fig. 3B). A nomogram was then constructed to predict the risk of N-HCC in patients based on GPC3 (score: 0=0, 1=39), PIVKA-II (score: 0=0, 1=100), and GGT (score: 0=0, 1=49) (Fig. 3C).

We conducted ROC analysis on the nomogram prediction model in both training and validation cohorts. The AUC values in each cohort were 0.937 (95%CI: 0.895–0.978) and 0.955(95%CI: 0.914–0.997), respectively (Fig. 3D). The calibration curve analysis for the nomogram proved an excellent agreement between predicted N-BLD and N-HCC statuses for both the training and validation cohorts (Fig. 3E and F). This suggests no deviation from an ideal fit. DCA demonstrated that the nomogram offers a superior net benefit for predicting N-HCC compared to the “treat all or none” strategy across the majority of risk thresholds (Fig. 3G and H).

Further, The AUC in the nomogram prediction models was 0.943 (95%CI: 0.912–0.974) (Fig. 3I). The cutoff value of 73.338 for the nomogram prediction model in diagnosing N-HCC resulted in a sensitivity of 95.20%, a specificity of 81.70%, and an accuracy of 76.90% (Table 3). The nomogram prediction model demonstrated superior sensitivity for stage I tumors (94.60%), showing statistically significant differences compared to GPC3 (86.49%) and PIVKA-II (83.78%) (Table 3). Similarly, in the assessment of tumors smaller than 3 cm, the nomogram prediction model exhibited significantly higher sensitivity (93.10%) than both GPC3 (72.41%) and PIVKA-II (79.31%) (Table 3).

Relationship between GPC3 and PIVKA-II expression levels and patient survival

Among the 104 N-HCC patients, 31 (29.81%) underwent surgical resection, while the remaining 73 (70.19%) received non-surgical interventions, including transcatheter arterial chemoembolization (TACE), radiofrequency ablation (RFA), and supportive care. With a follow-up through March 2023, 53 patients (50.96%) achieved 3-year overall survival (OS).

The association between biomarker levels and OS was analyzed using RCS method with 3 knots positioned at the 10th, 50th, and 90th percentiles. A significant nonlinear relationship was observed between GPC3 levels and OS (nonlinear $P<0.05$). Specifically, when GPC3 concentrations exceeded the median level of 0.124 ng/mL (HR = 1.000; 95%CI: 0.995–1.009), a rapid increase in all-cause mortality risk was evident (Fig. 4A). Similarly, PIVKA-II levels demonstrated a nonlinear association with OS (nonlinear $P<0.05$), with a marked elevation in mortality risk observed beyond the median level of 274 mAU/mL (HR = 1.000; 95%CI: 0.981–1.004) (Fig. 4B).

Using established survival cutoff values, patients were stratified into high-risk and low-risk groups for both biomarkers. Significant associations were observed between these risk stratifications and survival outcomes, including both survival duration and rate ($P<0.05$; Fig. 4C and D). Comparative analysis revealed that the GPC3-highrisk group exhibited significantly reduced OS rates at 1-, 2-, and 3-year intervals compared to the low-risk group ($P<0.05$; Table 4).

A nomogram prognosis prediction model for OS in patients with N-HCC was developed

The GPC3-highrisk group exhibited significant correlations with larger tumor size (HCC > 5 cm) and distant metastasis. However, no significant associations were observed with factors such as age, gender, cirrhosis, chronic hepatitis B (CHB), portal vein thrombosis (PVT), tumor multiplicity, intrahepatic metastasis, ascites, or serum albumin (ALB) and total bilirubin (TBIL) levels (all with $P>0.05$). Similarly, the PIVKA-II-highrisk group showed significant relationships with age, gender, PVT, tumor size and number, intrahepatic metastasis, and ascites, but not with cirrhosis, CHB, distant metastasis, or ALB and TBIL levels (all with $P>0.05$; Table 5). To further evaluate the correlation between all parameters and OS rate, univariate logistic regression analysis was conducted. The results identified 14 parameters

Table 3 Comparative diagnostic metrics for GPC3, PIVKA-II and nomogram diagnostic prediction model

Variables	Sensitivity	Specificity	PPV	NPV	Accuracy	Sensitivity (Stage I)	Sensitivity (< 3 cm)
GPC3	76.92%	73.08%	74.07%	76.00%	50.00% ^a	86.49% ^c	72.41% ^e
PIVKA-II	84.62%	90.38%	89.80%	85.45%	75.00% ^b	83.78% ^d	79.31% ^f
Nomogram	95.20%	81.70%	83.90%	94.40%	76.90%	94.60%	93.10%
<i>P</i> value	0.001	0.008	0.010	0.002	0.000	0.036	0.001

GPC3, detectable serum GPC3, at a cut-off value of 0.100 ng/mL

PIVKA-II, detectable serum PIVKA-II, at a cut-off value of 40.00 mAU/mL

Nomogram, the scores of the variables including GPC3 (score: 0 = 0, 1 = 36), PIVKA-II (score: 0 = 0, 1 = 100), and GGT (score: 0 = 0, 1 = 56) were calculated, followed by determining the positions of each variable on the related axis. Vertical lines were then drawn on each axis, and the corresponding scores were found. Each variable's score was further added to obtain the total score, at a cut-off value of 73.338

PPV, positive predictive value; NPV, negative predictive value

Three variables were compared by the chi-square test or Fisher's exact test and $P < 0.05$ was statistically significant. a: Nomogram vs. GPC3 in accuracy, $P = 0.000$

b: Nomogram vs. PIVKA-II in accuracy, $P = 0.741$

c: Nomogram vs. GPC3 in sensitivity (Stage I), $P = 0.030$

d: Nomogram vs. PIVKA-II in sensitivity (Stage I), $P = 0.011$

e: Nomogram vs. GPC3 in sensitivity (< 3 cm), $P = 0.000$

f: Nomogram vs. PIVKA-II in sensitivity (< 3 cm), $P = 0.003$

as influencing factors on the OS rate, including GPC3-highrisk, PIVKA-II-highrisk, PVT, CHB, cirrhosis, tumor size, daughter nodule, intrahepatic metastasis, distant metastasis, ascites, presence of symptoms, ALB below 40 g/L, TBIL above 21 $\mu\text{mol/L}$, and surgical therapy (all with $P < 0.1$, Fig. 5A).

Next, we used the LASSO regression method to filter the model parameters and reduce complexity to address the overfitting problem (Fig. 5B). Following this, a step-wise Cox regression analysis based on the Akaike Information Criterion (AIC) was conducted, resulting in the identification of 10 optimal parameters for establishing the prognostic model. These parameters encompassed GPC3-high risk, PVT, CHB, cirrhosis, intrahepatic metastasis, ascites detected by symptoms, ALB levels below 40 g/L, TBIL levels above 21 $\mu\text{mol/L}$, and surgical therapy (Fig. 5C). Multivariate Cox proportional risk regression analysis revealed that GPC3-highrisk, cirrhosis, PVT, and ALB level < 40 g/L were independent risk factors affecting OS rate and prognosis, whereas surgical therapy was an independent protective factor (Fig. 5D).

Based on these findings, a nomogram prognosis prediction model was constructed using the 5 parameters selected by multivariate Cox proportional risk regression analysis to predict individual prognosis (Fig. 5E). In this nomogram, scores were assigned to each variable: GPC3-highrisk (score: 0 = 0, 1 = 51), cirrhosis (score: 0 = 0, 1 = 41), PVT (score: 0 = 0, 1 = 86), ALB level < 40 g/L (score: 0 = 0, 1 = 34), and surgery (score: 0 = 100, 1 = 0). The total score was calculated by summing the scores of each variable, and the total fractal axis was used to predict the death probability of a given patient with N-HCC. For instance, a patient with preoperative ALB < 40 g/L, GPC3 > 0.124 ng/mL, PVT, and undergoing TACE but without cirrhosis had a total survival score of 271, with an estimated 12-month survival probability of

approximately 40% and a 24-month survival probability of approximately 10%.

To evaluate and optimize model performance, cross-validation, bootstrap, and other methods were utilized. The AUCs of the prognostic nomogram scoring system for predicting survival rates at 12, 24, and 36 months were 0.909 (95%CI: 0.843–0.975), 0.864 (95%CI: 0.789–0.940), and 0.871 (95%CI: 0.803–0.929), respectively (Fig. 5F). The calibration chart demonstrated a good match between the predicted and actual probabilities (Fig. 5G). Resampling internal verification using the bootstrap method also indicated acceptable accuracy of the scoring model (Fig. 5H). Finally, using individual nomogram scores, patients were divided into 2 groups based on a median value of 177.66, and a significant correlation was detected between nomogram scores and the survival time and rate of the patients ($P < 0.0001$; Fig. 5I).

Discussion

Despite ongoing debates and limitations surrounding serological diagnostic and monitoring approaches for HCC, AFP persists as a widely utilized parameter in clinical diagnosis and treatment of this hepatic malignancy [22, 31]. Previous investigations have consistently indicated that the pathogenesis and progression mechanisms of N-HCC may substantially differ from those of typical HCC cases [35, 36], a finding that aligns with our current study results. Utilizing the established serum cutoff value of 20 ng/mL for AFP, our analysis revealed that N-HCC patients comprised 25.3% of the total HCC population. Notably, the N-HCC group exhibited a significantly higher proportion of patients who were older, male, and presented with stage I disease, smaller tumor size, and non-metastatic characteristics compared to the A-HCC group. These distinctive features render N-HCC particularly susceptible to being overlooked in clinical practice.

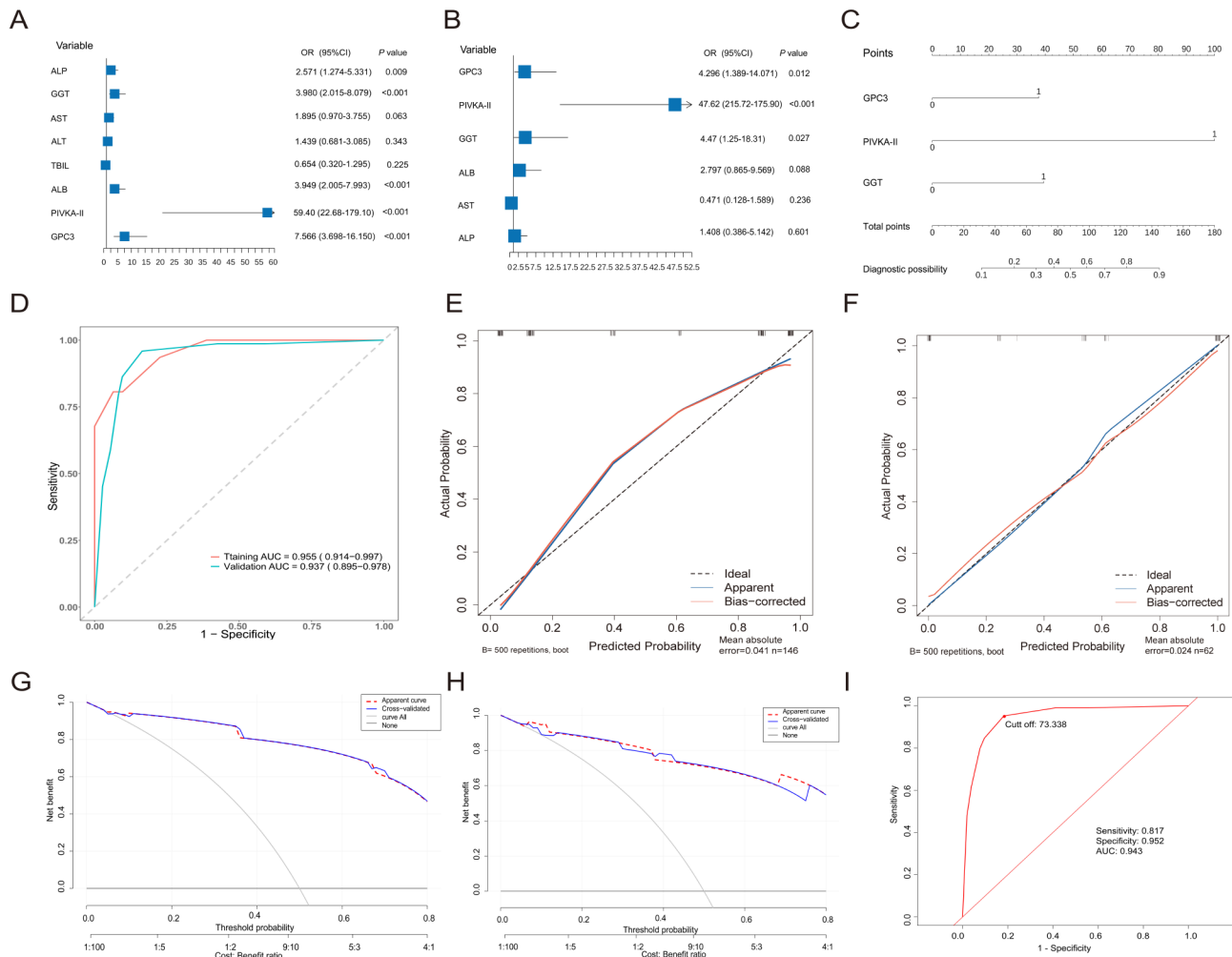


Fig. 3 Stepwise identification of pivotal parameters of the model and development and validation of a nomogram diagnostic prediction model. **(A)** 6 parameters were risk factors of patients with HCC by univariate Logistic analysis. **(B)** 3 parameters were risk factors of patients with HCC by multivariate Logistic analysis. **(C)** Establishment of nomogram score based on 3 parameters. **(D)** ROC curves of the prediction model in the modeling group and validation group. **(E)** Calibration chart of the prediction model in the modeling group. **(F)** Calibration chart of the prediction model in the validation group. **(G)** DCA curves of the prediction model in the modeling group. **(H)** DCA curve analysis evaluating the prediction model's net benefit in the validation cohort. **(I)** ROC curves of the prediction model

Consequently, the implementation of effective early screening and diagnostic strategies for N-HCC patients may prove pivotal in enhancing the overall prognosis of the HCC population.

Several chronic liver diseases, including chronic hepatitis, autoimmune hepatitis, and alcoholic hepatitis, can progress to cirrhosis, which represents a major predisposing factor for HCC development [37]. It is noteworthy that while the majority of HCC cases arise from chronic hepatitis or cirrhosis or both, not all cases of cirrhosis inevitably progress to HCC [21]. The distinctive feature of the present study, compared to previous investigations, lies in its utilization of AFP-negative CHB and cirrhosis cases (primarily cirrhosis) as controls in this case-control study design. Demographic and clinical characteristics, including cirrhosis prevalence, hepatitis B virus status,

and Child-Pugh classification, were carefully matched between the two groups. Through this approach, we were able to precisely and comprehensively assess the accuracy of GPC3 and PIVKA-II in the differential diagnosis between the 2 groups.

GPC3 and PIVKA-II, both implicated in critical cellular processes including cell growth, differentiation, and migration, have been shown to exhibit expression levels in HCC that are positively correlated with tumor size [15, 23, 28]. Our current study findings are consistent with this observation, demonstrating that GPC3 and PIVKA-II concentrations progressively increase with larger tumor dimensions. Interestingly, although GPC3 and PIVKA-II expression levels in stage IV N-HCC were significantly elevated compared to those in stage I, no significant association was observed between their expression

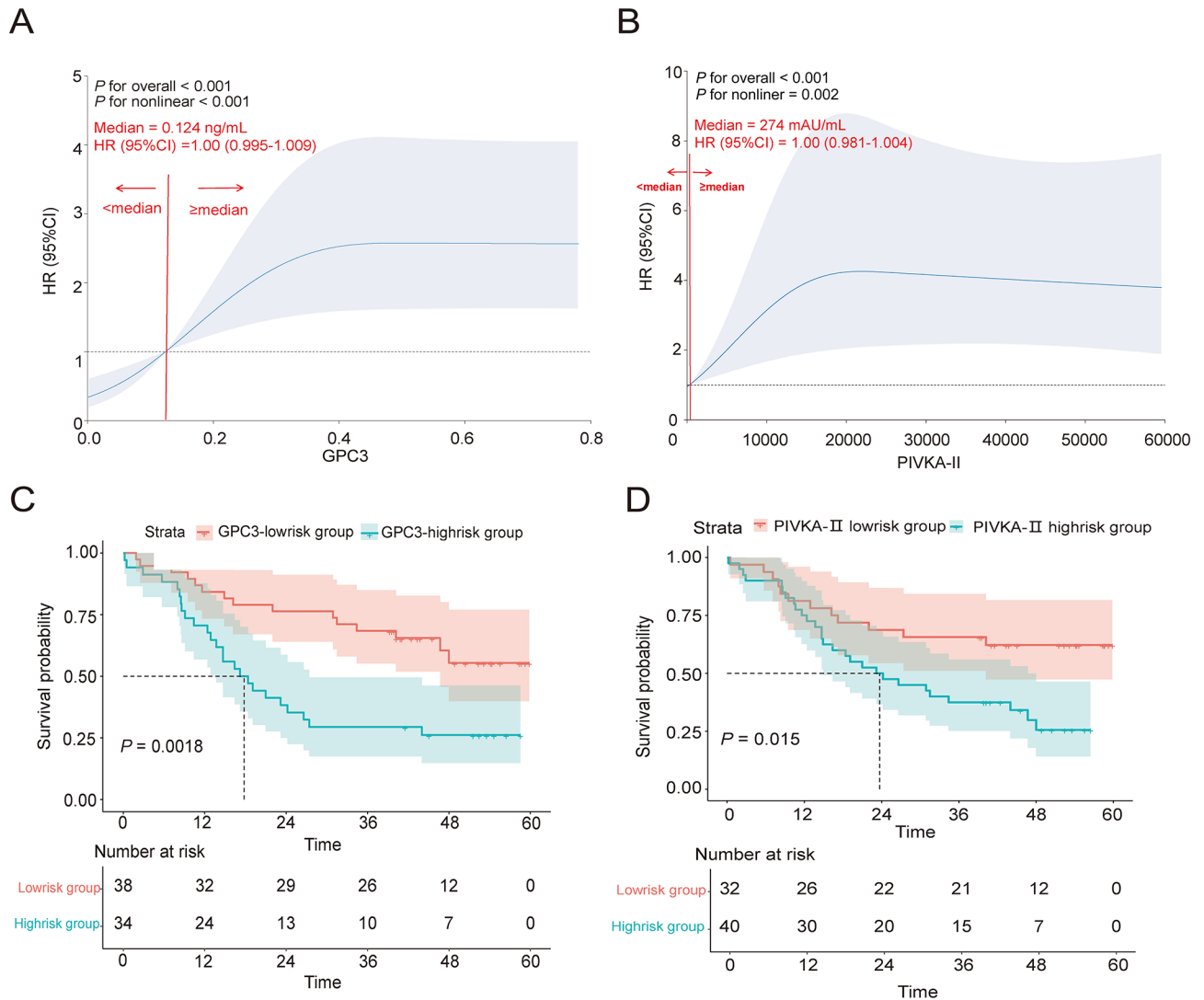


Fig. 4 Restriction cubic spline of GPC3 and PIVKA-II expression level and survival examination of N-HCC patients. **(A)** Restriction cubic spline of GPC3 level. **(B)** Restriction cubic spline of PIVKA-II level. **(C)** Survival curve corresponding to GPC3 expression level alterations. **(D)** Survival curve associated with PIVKA-II expression level modifications

Table 4 Comparative analysis of annual survival rates of HCC-N patients based on risk stratification of GPC3 and PIVKA-II

Groups	Number	Median survival (month)	1-year OS, n(%)	2-year OS, n(%)	3-year OS, n(%)
GPC3-lowrisk (≤ 0.124 ng/mL)	54	42.473	47 (87.04%)	41 (75.93%)	34 (62.96%)
GPC3-highrisk (> 0.124 ng/mL)	50	28.165	35 (70.00%)	22 (44.00%)	19 (38.00%)
P value		0.002	0.034	0.001	0.011
PIVKA-II-lowrisk (≤ 274 mAU/mL)	53	40.007	44 (83.02%)	35 (66.04%)	32 (60.38%)
PIVKA-II-highrisk (> 274 mAU/mL)	51	30.125	38 (74.51%)	28 (54.90%)	21 (41.18%)
P value		0.028	0.288	0.245	0.050

GPC3, detectable serum GPC3; PIVKA-II, detectable serum PIVKA-II; OS, overall survival

GPC3-lowrisk vs. GPC3-highrisk, were compared by the chi-square test or Fisher's exact test and $P < 0.05$ was statistically significant

PIVKA-II-lowrisk vs. PIVKA-II-highrisk, were compared by the chi-square test or Fisher's exact test and $P < 0.05$ was statistically significant

Table 5 Analysis of the correlation between risk stratification of GPC3 and PIVKA-II and the clinical features of HCC

Clinical features	Number	GPC3-highrisk (> 0.124 ng/mL)	OR (95%CI)	P value	PIVKA-II-highrisk (> 274mAU/mL)	OR (95%CI)	P value
Age, n(%)							
≤ 60 years	52	26 (50.00%)	1.167 (0.540–2.519)	0.695	32 (61.54%)	2.779 (1.256–6.149)	0.011
> 60 years	52	24 (46.15%)			19 (36.54%)		
Gender, n(%)							
Male	96	45 (46.88%)	0.529 (0.120–2.341)	0.395	50 (52.08%)	7.609 (0.901–64.232)	0.031
Female	8	5 (62.50%)			1 (12.5%)		
Cirrhosis, n(%)							
Yes	70	33 (47.14%)	0.892 (0.393–2.025)	0.784	36 (51.43%)	1.341 (0.589–3.055)	0.484
No	34	17 (50.00%)			15 (44.11%)		
Hepatitis B virus, n(%)							
Yes	92	43 (46.74%)	0.627 (0.185–2.120)	0.450	47 (51.09%)	2.089 (0.588–7.423)	0.247
No	12	7 (58.33%)			4 (33.33%)		
PVT, n(%)							
Yes	45	24 (53.33%)	1.451 (0.665–3.162)	0.349	29 (64.44%)	3.048 (1.360–6.831)	0.006
No	59	26 (44.07%)			22 (37.29%)		
Tumor size, n(%)							
< 3 cm	29	12 (41.38%)	2.511 (2.036–2.986)	0.034	4 (13.79%)	3.144 (2.720–3.568)	0.000
3–5 cm	42	16 (38.10%)			22 (52.38%)		
> 5 cm	33	22 (66.67%)			25 (75.76%)		
Daughter nodule, n(%)							
Yes	45	26 (57.78%)	0.501 (0.228–1.101)	0.084	29 (64.44%)	0.328 (0.146–0.735)	0.006
No	59	24 (40.68%)			22 (37.29%)		
Intrahepatic metastasis, n(%)							
Yes	34	19 (55.88%)	1.594 (0.698–3.636)	0.267	25 (73.53%)	4.701 (1.905–11.598)	0.000
No	70	31 (44.29%)			26 (37.14%)		
Distant metastasis, n(%)							
Yes	18	14 (77.78%)	4.861 (1.477–15.994)	0.006	10 (55.56%)	1.372 (0.494–3.810)	0.543
No	86	36 (41.86%)			41 (47.67%)		
Ascites, n(%)							
Yes	35	19 (54.29%)	1.456 (0.643–3.295)	0.367	23 (65.71%)	2.807 (1.203–6.549)	0.015
No	69	31 (44.93%)			28 (40.58%)		
ALB, n(%)							
40–55 g/L	35	15 (42.86%)	0.729 (0.321–1.653)	0.448	15 (42.86%)	0.688 (0.303–1.560)	0.369
< 40 g/L	69	35 (50.72%)			36 (52.17%)		
TBIL, n(%)							
5–21 μmol/L	74	35 (47.30%)	0.897 (0.384–2.097)	0.803	37 (50.00%)	1.143 (0.489–2.673)	0.758
> 21 μmol/L	30	15 (50.00%)			14 (46.67%)		

CHB, Chronic Hepatitis B. PVT, portal vein thrombosis. ALB, albumin. TBIL, total bilirubin

Categorical variables were compared by the chi-square test or Fisher's exact test and $P < 0.05$ was statistically significant

levels and TNM staging in N-HCC. This discrepancy may be attributed to several factors, including the secretion mechanisms of these biomarkers, tumor biology, the multidimensional nature of staging assessments, and limitations in detection methodologies. Furthermore, our study revealed that GPC3 and PIVKA-II expression levels in stage I N-HCC or tumor size < 3 cm were significantly higher than those in the N-BLD group. These findings highlight the clinical significance of monitoring longitudinal changes in the levels of these 2 biomarkers, which could significantly improve the early detection rate

of stage I and small HCC, ultimately leading to enhanced patient survival outcomes.

The current research on the diagnostic utility of GPC3 predominantly employs ROC analysis to determine diagnostic cutoff values, which have demonstrated significant variability across studies. A comprehensive meta-analysis of these studies revealed a pooled sensitivity of 55% and specificity of 58% (AUC: 0.7793) [21]. In a pivotal investigation, an optimized cutoff value of 0.02 ng/mL was established for the early detection and diagnosis of N-HCC, demonstrating a sensitivity of 57.70% while maintaining perfect specificity at 100% [13]. In our study,

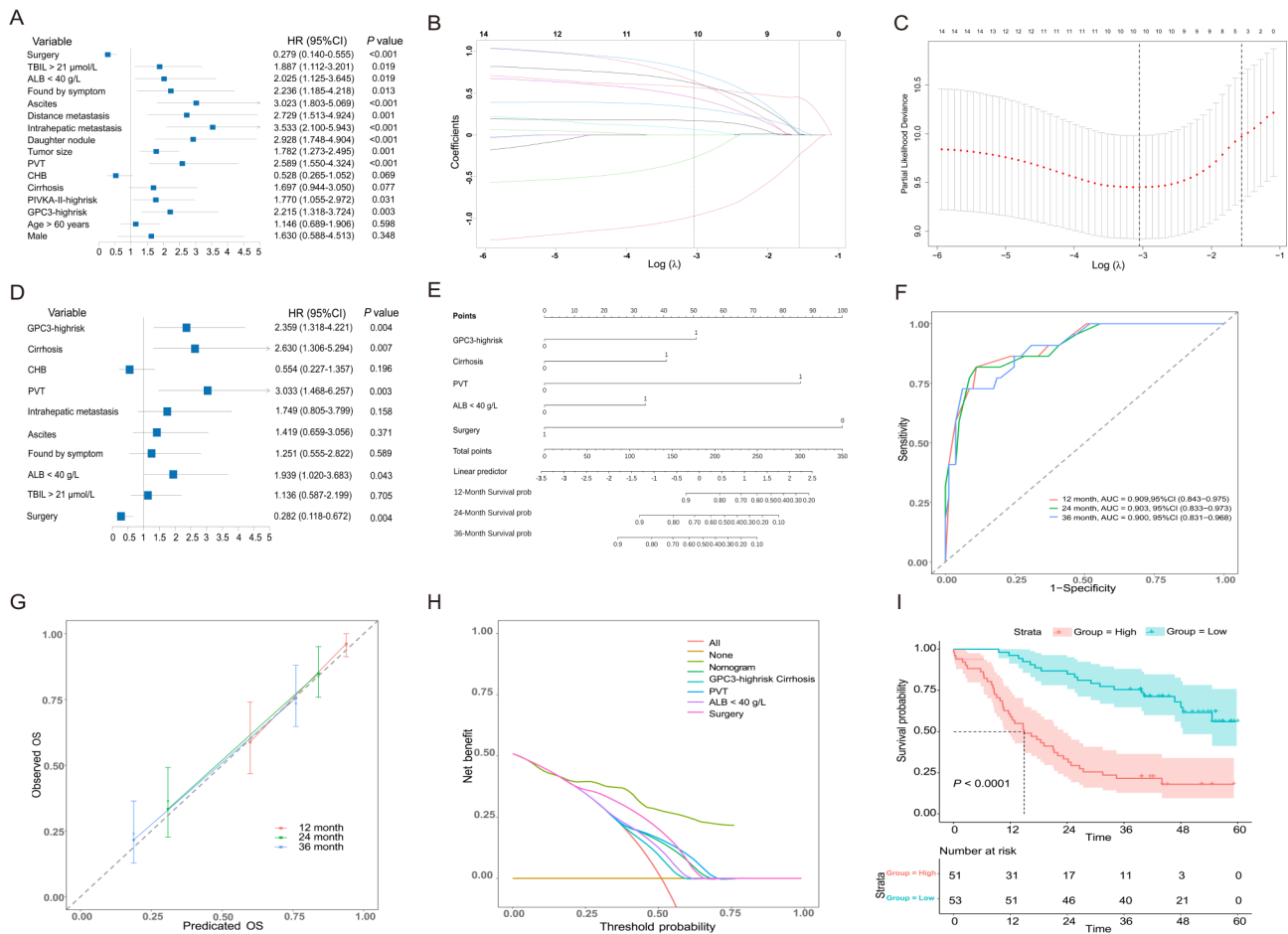


Fig. 5 Development and validation of a nomogram prognosis prediction model. **(A)** 14 parameters profoundly associated with the overall survival (OS) of patients with HCC by univariate Cox regression analysis. **(B)** LASSO coefficient profiles of the clinical features. **(C)** The optimal penalization coefficient lambda was generated in the LASSO via tenfold cross-validation. We plotted the partial likelihood deviance (binomial deviance) curve versus log(lambda) and drew dotted vertical lines based on 1 standard error criteria. **(D)** 5 parameters profoundly associated with the OS of patients with HCC by multivariate Cox regression analysis. **(E)** Establishment of nomogram score based on 5 parameters. **(F)** ROC curves of the prediction model for predicting the survival rates at 12, 24, and 36 months. **(G)** The consistency index (Concordance Index, C-index) appraises the model differentiation degree for predicting the survival rates at 12, 24, and 36 months. **(H)** DCA curves of the prediction model. **(I)** Survival curve corresponding to nomogram score expression alterations

utilizing a serum cutoff value of 0.100 ng/mL determined through ROC analysis (AUC: 0.751), GPC3 exhibited a sensitivity of 76.92% for N-HCC diagnosis and a specificity of 73.08% for distinguishing N-HCC from N-BLD. This relatively high specificity might have potential utility as a complementary biomarker to increase the sensitivity of other N-HCC biomarkers, alone or in combination.

PIVKA-II, an inactive prothrombin precursor primarily synthesized in the liver under conditions of vitamin K deficiency, exhibits no significant correlation with AFP levels [27, 28, 30]. A comprehensive meta-analysis revealed that the majority of studies adopted a PIVKA-II cutoff value of 40 mAU/mL [38]. In our study, utilizing this established cutoff value for N-HCC identification demonstrated a sensitivity of 84.62%, specificity of 90.38%, and an AUC of 0.925. These findings suggest that PIVKA-II demonstrates superior diagnostic efficacy

compared to GPC3 in distinguishing N-HCC cases. In the current study, we also developed and validated a nomogram-based prediction model incorporating GPC3, PIVKA-II, and liver function indicators, specifically utilizing three serological indices: GPC3, PIVKA-II, andGGT. Following comprehensive evaluation of the model's discrimination, calibration, and clinical validity, our results demonstrate that this model exhibits significant clinical utility and interpretability. The nomogram prediction model, utilizing a cutoff value of 73.542 for N-HCC diagnosis, demonstrated superior diagnostic performance with a sensitivity of 95.20%, specificity of 81.70%, and an AUC of 0.943. The prediction model, which incorporates only 3 serum indicators that can be readily obtained upon hospital admission for hepatopathy patients, represents a potentially valuable tool for identifying individuals at high risk of N-HCC within 48 h

of admission. In clinical practice, adopting this model helps to improve the diagnostic accuracy of the N-HCC.

Previous studies have suggested that plasma GPC3 levels may serve as a valuable biomarker for identifying patients at high risk of HCC recurrence following surgical resection, particularly in early-stage disease [39]. Moreover, key prognostic indicators for HCC have been identified, encompassing bilirubin, albumin, AFP-L3, AFP, and PIVKA-II [40]. In this study, we innovatively employed a three-node restricted cubic spline analysis to develop a flexible and visually interpretable predictive model. Our findings not only revealed a significant nonlinear relationship between the 2 markers and OS but also established cutoff values for GPC3 and PIVKA-II to stratify patients into distinct risk groups. These risk stratifications demonstrated significant associations with survival outcomes, including both survival duration and rates.

This study further investigated whether these risk stratifications were associated with other HCC prognostic factors, including tumor size, the presence or absence of PVT, and liver-related factors such as serum bilirubin, ALB, and transaminase levels [40, 41]. Current research on the association between the 2 markers (GPC3 and PIVKA-II) and prognostic-related factors has demonstrated significant variability across studies [42, 43]. Our analysis revealed that the GPC3-highrisk group was significantly associated with tumor size and distant metastasis but not with other clinical features. In contrast, the PIVKA-II-highrisk group was associated with multiple prognostic factors. Although univariate analysis indicated that high-risk levels of both markers were correlated with HCC prognosis, LASSO regression and multivariate Cox regression analyses demonstrated that only the GPC3-highrisk level was an independent risk factor affecting OS rates and poor patient prognosis. This may be due to the difficulty in distinguishing the independent effects of these variables in the multivariate analysis when the independent variables are highly correlated.

Furthermore, when constructing the nomogram prognosis prediction model using independent prognostic factors identified through multivariate Cox regression analysis, we found that the model incorporated 4 independent risk factors and one independent protective factor related to surgical therapy. As is well-established, hepatectomy remains the primary treatment for HCC, and the efficacy of this surgical resection technique has significantly improved the 5-year OS rate to approximately 30–60% [44]. The 4 independent risk factors, GPC3-highrisk, cirrhosis, PVT, and ALB levels, can be readily assessed through imaging examinations and serological tests prior to treatment initiation. Our findings demonstrated that this nomogram prognosis prediction model effectively distinguished between high- and

low-risk patients with N-HCC. Moreover, it confirmed that the OS prognosis in the high-risk group was significantly worse compared to the low-risk group. Therefore, this nomogram prognosis prediction model perhaps represents a valuable clinical tool for helping clinicians judge and selection of optimal therapeutic strategies based on individual patient risk profiles.

This study has several limitations. First, the nomogram has not been externally validated. We plan to address this by continuously recruiting patients from third-party sources to complete external validation. Second, during the construction of the prognostic prediction model, we considered that splitting the sample might affect model fitting. Therefore, we avoided data splitting and instead utilized cross-validation, bootstrap methods, and regularization techniques to evaluate and optimize model performance. These approaches were implemented to mitigate overfitting and ensure the model's generalization ability. In the future, we aim to expand the sample size to further validate the model's robustness. Third, we did not analyze the changes in GPC3 and PIVKA-II levels before and after treatment, nor did we explore the correlation between post-treatment levels and prognosis. We intend to investigate these aspects in future studies.

Conclusions

In conclusion, our study revealed that serological models could serve as valuable tumor markers for N-HCC by providing good differential diagnosis, early diagnosis, thereby presenting a solid basis for patient prognosis. However, this study has a few limitations, including an insufficient number of patients with N-HCC in the examined population of 2 medical centers and the absence of large samples to verify and evaluate the prognosis of the nomogram scoring model. Therefore, we will expand the study sample size to verify the accuracy of our nomogram prognostic scoring model in future studies.

Acknowledgements

We thank Bullet Edits Limited for the linguistic editing and proofreading of the manuscript.

Author contributions

Yingying Lin, Zhaolei Cui and Zhenzhou Xiao designed the study; Yuefei Ma, Yan Chen, Jinchuan Lin, and Yeppei Huang collected the literature and conducted the analysis of pooled data; Yingying Lin wrote the manuscript; Yuefei Ma helped to draft the manuscript; Zhaolei Cui and Zhenzhou Xiao proofread, revised and final approved the manuscript; all authors have approved the version to be published.

Funding

This study was supported by the Provincial Natural Science Fund of Fujian (Grant numbers: 2021J01439, 2023J011294), Fujian Provincial Health Technology Project (Grant number: 2021GGA047), Joint Funds for the Innovation of Science and Technology, Fujian province (Grant number: 2024Y9609), and the Outstanding Young Talent Program of Fujian Cancer Hospital (2020YNYQ07).

Data availability

The datasets used and/or analyzed during the current study are available from the corresponding author upon reasonable request.

Declarations**Ethics approval and consent to participate**

The study was approved by the Ethics Review Board of the Branch for Research and Clinical Technology Application, Ethics Committee of the Fujian Cancer Hospital (Approval No. SQ2015-049-01) and the First Affiliated Hospital of Fujian Medical University (Approval No. MRCTA, ECFAH of FMU [2017]019), and the study was conducted in compliance with the principle of the Declaration of Helsinki. Written informed consent was obtained from all patients or their family members.

Consent for publication

Not applicable.

Competing interests

The authors declare no competing interests.

Author details

¹Laboratory of Biochemistry and Molecular Biology Research, Department of Clinical Laboratory, Clinical Oncology School of Fujian Medical University, Fujian Cancer Hospital, Fuzhou 350014, Fujian, China
²Department of Laboratory Medicine, the First Affiliated Hospital, Fujian Medical University, Fuzhou 350005, China
³Department of Laboratory Medicine, National Regional Medical Center, Binhai Campus of the First Affiliated Hospital, Fujian Medical University, Fuzhou 350212, China

Received: 1 November 2023 / Accepted: 26 March 2025

Published online: 17 April 2025

References

- Huang DQ, Singal AG, Kono Y, Tan DJH, El-Serag HB, Loomba R. Changing global epidemiology of liver cancer from 2010 to 2019: NASH is the fastest growing cause of liver cancer. *Cell Metabol.* 2022;34(7):969–e977962.
- Bray F, Laversanne M, Sung H, Ferlay J, Siegel RL, Soerjomataram I, Jemal A. Global cancer statistics 2022: GLOBOCAN estimates of incidence and mortality worldwide for 36 cancers in 185 countries. *Cancer J Clin.* 2024;74(3):229–63.
- Mai RY, Wang YY, Bai T, Chen J, Xiang BD, Wu GB, Wu FX, Li LQ, Ye JZ. Combination of ALBI and APRI to predict Post-Hepatectomy liver failure after liver resection for HBV-Related HCC patients. *Cancer Manage Res.* 2019;11:8799–806.
- Bartolomeo N, Trerotoli P, Serio G. Progression of liver cirrhosis to HCC: an application of hidden Markov model. *BMC Med Res Methodol.* 2011;11:38.
- Kim BH, Lim YS, Kim EY, Kong HJ, Won YJ, Han S, Park S, Hwang JS. Temporal improvement in survival of patients with hepatocellular carcinoma in a hepatitis B virus-endemic population. *J Gastroenterol Hepatol.* 2018;33(2):475–83.
- Sherman M. Hepatocellular carcinoma: screening and staging. *Clin Liver Dis.* 2011;15(2):323–34. vii-x.
- Allemani C, Matsuda T, Di Carlo V, Harewood R, Matz M, Nikšić M, Bonaventure A, Valkov M, Johnson CJ, Estève J, et al. Global surveillance of trends in cancer survival 2000–14 (CONCORD-3): analysis of individual records for 37 513 025 patients diagnosed with one of 18 cancers from 322 population-based registries in 71 countries. *Lancet (London England).* 2018;391(10125):1023–75.
- Tzartzeva K, Singal AG. Testing for AFP in combination with ultrasound improves early liver cancer detection. *Expert Rev Gastroenterol Hepatol.* 2018;12(10):947–9.
- Chakraborty E, Sarkar D. Emerging therapies for hepatocellular carcinoma (HCC). *Cancers (Basel).* 2022;14(11):2798.
- Galle PR, Foerster F, Kudo M, Chan SL, Llovet JM, Qin S, Schelman WR, Chintharlapalli S, Abada PB, Sherman M, et al. Biology and significance of alpha-fetoprotein in hepatocellular carcinoma. *Liver International: Official J Int Association Study Liver.* 2019;39(12):2214–29.
- Hughes DM, Berhane S, Emily de Groot CA, Toyoda H, Tada T, Kumada T, Satomura S, Nishida N, Kudo M, Kimura T, et al. Serum levels of α -Fetoprotein increased more than 10 years before detection of hepatocellular carcinoma. *Clin Gastroenterol Hepatology: Official Clin Pract J Am Gastroenterological Association.* 2021;19(1):162–e170164.
- Capurro M, Wanless IR, Sherman M, Deboer G, Shi W, Miyoshi E, Filmus J. Glypican-3: a novel serum and histochemical marker for hepatocellular carcinoma. *Gastroenterology.* 2003;125(1):89–97.
- Lee CW, Tsai HI, Lee WC, Huang SW, Lin CY, Hsieh YC, Kuo T, Chen CW, Yu MC. Normal Alpha-Fetoprotein hepatocellular carcinoma: are they really normal? *J Clin Med.* 2019;8(10):1736.
- Bruix J, Sherman M. Management of hepatocellular carcinoma: an update. *Hepatology (Baltimore MD).* 2011;53(3):1020–2.
- Zheng X, Liu X, Lei Y, Wang G, Liu M. Glypican-3: A novel and promising target for the treatment of hepatocellular carcinoma. *Front Oncol.* 2022;12:824208.
- Zhou F, Shang W, Yu X, Tian J. Glypican-3: A promising biomarker for hepatocellular carcinoma diagnosis and treatment. *Med Res Rev.* 2018;38(2):741–67.
- Tsuchiya N, Sawada Y, Endo I, Saito K, Uemura Y, Nakatsura T. Biomarkers for the early diagnosis of hepatocellular carcinoma. *World J Gastroenterol.* 2015;21(37):10573–83.
- Anatelli F, Chuang ST, Yang XJ, Wang HL. Value of glypican 3 immunostaining in the diagnosis of hepatocellular carcinoma on needle biopsy. *Am J Clin Pathol.* 2008;130(2):219–23.
- Jing JS, Ye W, Jiang YK, Ma J, Zhu MQ, Ma JM, Zhou H, Yu LQ, Yang YF, Wang SC. The value of GPC3 and GP73 in clinical diagnosis of hepatocellular carcinoma. *Clin Lab.* 2017;63(11):1903–9.
- Wu M, Liu Z, Zhang A, Li N. Associated measurement of fucosylated levels of AFP, DCP, and GPC3 for early diagnosis in hepatocellular carcinoma. *Int J Biol Mark.* 2019;34(1):20–6.
- Xu D, Su C, Sun L, Gao Y, Li Y. Performance of serum glypican 3 in diagnosis of hepatocellular carcinoma: A meta-analysis. *Ann Hepatol.* 2019;18(1):58–67.
- Johnson P, Zhou Q, Dao DY, Lo YMD. Circulating biomarkers in the diagnosis and management of hepatocellular carcinoma. *Nat Reviews Gastroenterol Hepatol.* 2022;19(10):670–81.
- Yu JP, Xu XG, Ma RJ, Qin SN, Wang CR, Wang XB, Li M, Li MS, Ma Q, Xu WW. Development of a clinical chemiluminescent immunoassay for serum GPC3 and simultaneous measurements alone with AFP and CK19 in diagnosis of hepatocellular carcinoma. *J Clin Lab Anal.* 2015;29(2):85–93.
- Ozkan H, Erdal H, Koçak E, Tutkak H, Karaeren Z, Yakut M, Köklü S. Diagnostic and prognostic role of serum glypican 3 in patients with hepatocellular carcinoma. *J Clin Lab Anal.* 2011;25(5):350–3.
- Kudo M, Izumi N, Kokudo N, Matsui O, Sakamoto M, Nakashima O, Kojiro M, Makuuchi M. Management of hepatocellular carcinoma in Japan: Consensus-Based clinical practice guidelines proposed by the Japan society of hepatology (JSH) 2010 updated version. *Dig Dis (Basel Switzerland).* 2011;29(3):339–64.
- Prevention of hepatocellular carcinoma in the Asia-Pacific region: consensus statements. *J Gastroenterol Hepatol.* 2010;25(4):657–63.
- Gao P, Li M, Tian QB, Liu DW. Diagnostic performance of des- γ -carboxy prothrombin (DCP) for hepatocellular carcinoma: a bivariate meta-analysis. *Neoplasma.* 2012;59(2):150–9.
- Marrero JA, Feng Z, Wang Y, Nguyen MH, Befeler AS, Roberts LR, Reddy KR, Harnois D, Llovet JM, Normolle D, et al. Alpha-fetoprotein, des-gamma carboxyprothrombin, and lectin-bound alpha-fetoprotein in early hepatocellular carcinoma. *Gastroenterology.* 2009;137(1):110–8.
- Fujiyama S, Tanaka M, Maeda S, Ashihara H, Hirata R, Tomita K. Tumor markers in early diagnosis, follow-up and management of patients with hepatocellular carcinoma. *Oncology.* 2002;62(Suppl 1):57–63.
- Feng H, Li B, Li Z, Wei Q, Ren L. PIVKA-II serves as a potential biomarker that complements AFP for the diagnosis of hepatocellular carcinoma. *BMC Cancer.* 2021;21(1):401.
- Yang Y, Li G, Lu Z, Liu Y, Kong J, Liu J. Progression of prothrombin induced by vitamin K Absence-II in hepatocellular carcinoma. *Front Oncol.* 2021;11:726213.
- [Guidelines for diagnosis and treatment of primary liver cancer in China. (2019 edition)]. *Zhonghua gan zang bing za zhi = Zhonghua ganzangbing zazhi = Chinese. J Hepatol.* 2020;28(2):112–28.
- [The guidelines of prevention and treatment for chronic hepatitis B. (2019 version)]. *Zhonghua gan zang bing za zhi = Zhonghua ganzangbing zazhi = Chinese. Journal of hepatology* 2019;27(12):938–961.
- Xu XY, Ding HG, Li WG, Xu JH, Han Y, Jia JD, Wei L, Duan ZP, Ling-Hu EQ, Zhuang H. Chinese guidelines on the management of liver cirrhosis (abbreviated version). *World J Gastroenterol.* 2020;26(45):7088–103.

35. Samban SS, Hari A, Nair B, Kumar AR, Meyer BS, Valsan A, Vijayakurup V, Nath LR. An insight into the role of Alpha-Fetoprotein (AFP) in the development and progression of hepatocellular carcinoma. *Mol Biotechnol*. 2024;66(10):2697–709.
36. Zhao T, Jia L, Li J, Ma C, Wu J, Shen J, Dang L, Zhu B, Li P, Zhi Y, et al. Heterogeneities of Site-Specific N-Glycosylation in HCC tumors with low and high AFP concentrations. *Front Oncol*. 2020;10:496.
37. Llovet JM, Kelley RK, Villanueva A, Singal AG, Pikarsky E, Roayaie S, Lencioni R, Koike K, Zucman-Rossi J, Finn RS. Hepatocellular carcinoma. *Nat Reviews Disease Primers*. 2021;7(1):6.
38. De J, Shen Y, Qin J, Feng L, Wang Y, Yang L. A systematic review of Des- γ -Carboxy prothrombin for the diagnosis of primary hepatocellular carcinoma. *Medicine*. 2016;95(17):e3448.
39. Ofuji K, Saito K, Suzuki S, Shimomura M, Shirakawa H, Nobuoka D, Sawada Y, Yoshimura M, Tsuchiya N, Takahashi M, et al. Perioperative plasma glypican-3 level May enable prediction of the risk of recurrence after surgery in patients with stage I hepatocellular carcinoma. *Oncotarget*. 2017;8(23):37835–44.
40. Fox R, Berhane S, Teng M, Cox T, Tada T, Toyoda H, Kumada T, Kagebayashi C, Satomura S, Johnson PJ. Biomarker-based prognosis in hepatocellular carcinoma: validation and extension of the BALAD model. *Br J Cancer*. 2014;110(8):2090–8.
41. Carr BI, Pancoska P, Branch RA. Low alpha-fetoprotein hepatocellular carcinoma. *J Gastroenterol Hepatol*. 2010;25(9):1543–9.
42. Inagaki Y, Tang W, Makuuchi M, Hasegawa K, Sugawara Y, Kokudo N. Clinical and molecular insights into the hepatocellular carcinoma tumour marker des- γ -carboxyprothrombin. *Liver International: Official J Int Association Study Liver*. 2011;31(1):22–35.
43. Tangkijvanich P, Chanmee T, Komtong S, Mahachai V, Wisedopas N, Pothacharoen P, Kongtawelert P. Diagnostic role of serum glypican-3 in differentiating hepatocellular carcinoma from non-malignant chronic liver disease and other liver cancers. *J Gastroenterol Hepatol*. 2010;25(1):129–37.
44. Yarchoan M, Agarwal P, Villanueva A, Rao S, Dawson LA, Llovet JM, Finn RS, Groopman JD, El-Serag HB, Monga SP, et al. Recent developments and therapeutic strategies against hepatocellular carcinoma. *Cancer Res*. 2019;79(17):4326–30.

Publisher's note

Springer Nature remains neutral with regard to jurisdictional claims in published maps and institutional affiliations.